

Caging Metal Ions with Visible Light-Responsive Nanopolymersomes

Julianne C. Griepenburg,[†] Nimil Sood,[‡] Kevin B. Vargo,[‡] Dewight Williams,[§] Jeff Rawson,^{||} Michael J. Therien,^{||} Daniel A. Hammer,^{‡,†} and Ivan J. Dmochowski^{*,†}

[†]Department of Chemistry, University of Pennsylvania, 231 South 34th Street, Philadelphia, Pennsylvania 19104, United States

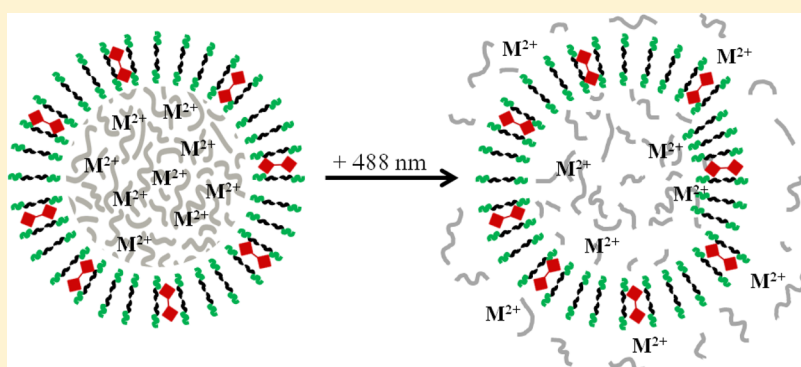
[‡]Department of Chemical and Biomolecular Engineering, University of Pennsylvania, 220 South 33rd Street, Philadelphia, Pennsylvania 19104, United States

[§]Department of Biochemistry and Biophysics, Perelman School of Medicine, University of Pennsylvania, 3700 Hamilton Walk, Philadelphia, Pennsylvania 19104, United States

^{||}Department of Chemistry, Duke University, 124 Science Drive, Durham, North Carolina 27708, United States

[†]Department of Bioengineering, University of Pennsylvania, 210 South 33rd Street, 240 Skirkanich Hall, Philadelphia, Pennsylvania 19104, United States

S Supporting Information



ABSTRACT: Polymersomes are bilayer vesicles that self-assemble from amphiphilic diblock copolymers, and provide an attractive system for the delivery of biological and nonbiological molecules due to their environmental compatibility, mechanical stability, synthetic tunability, large aqueous core, and hyperthick hydrophobic membrane. Herein, we report a nanoscale photoresponsive polymersome system featuring a *meso-to-meso* ethyne-bridged bis[(porphinato)zinc] (PZn_2) fluorophore hydrophobic membrane solute and dextran in the aqueous core. Upon 488 nm irradiation in solution or in microinjected zebrafish embryos, the polymersomes underwent deformation, as monitored by a characteristic red-shifted PZn_2 emission spectrum and confirmed by cryo-TEM. The versatility of this system was demonstrated through the encapsulation and photorelease of a fluorophore (FITC), as well as two different metal ions, Zn^{2+} and Ca^{2+} .

INTRODUCTION

The caging and precise spatiotemporal release of bioactive compounds is becoming increasingly important in the field of nanomedicine. A particular focus has been the development of chemical cages for metal ions, such as Zn^{2+} and Ca^{2+} . Zinc is required for normal cell function and important for both intracellular and extracellular signaling. Zinc deficiency can retard growth and lead to immunodeficiency.^{1–4} The biological importance of Ca^{2+} has been studied extensively in muscle contraction, cell signaling, gene regulation, thrombosis, wound healing, and cell death.⁵ Deficiencies in zinc and calcium are common in the human population, and can lead to neurological, cardiovascular, and endocrine disorders. Strategies for further probing the biological functions of these metal ions involve metal ion delivery to localized sites, which has the advantage of avoiding homeostatic disruption in nontarget areas.

Traditional approaches for caging metal ions have employed inorganic coordination chemistry, where one or more multivalent ligands coordinate the metal ion, and release of the caged ion is achieved by modulating the dissociation constant, K_D , for the ligand-metal ion complex. A family of ligands has been developed for Zn^{2+} and Ca^{2+} with weak and strong affinities.^{6–11} A common challenge with small-molecule ligands is the lack of specificity where similar ions can compete for binding to the coordination site. An extension of the thermodynamically driven release of metal ions is incorporation of stimulus responsiveness. Particularly attractive for applications that require targeted delivery of metal ions is the engineering of their release in response to light, as this can be

Received: September 20, 2014

Revised: December 1, 2014

Published: December 17, 2014

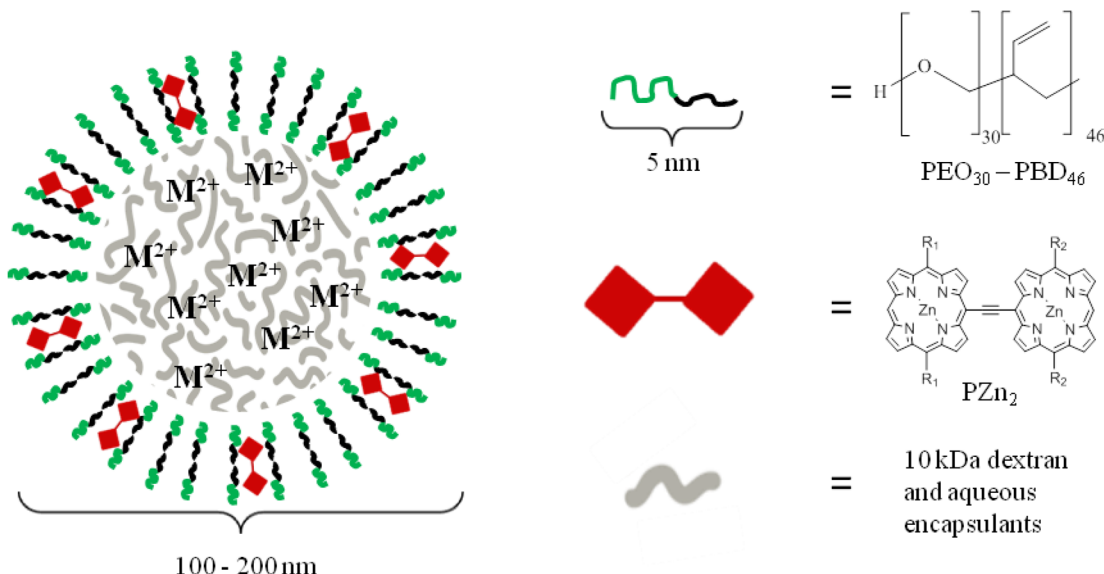


Figure 1. Photoresponsive nanopolymersome system. Nanopolymersomes were self-assembled from OB29 diblock copolymer ($\text{PEO}_{30}-\text{PBD}_{46}$). PZn_2 (Supporting Information) was encapsulated within the 10-nm-thick hydrophobic membrane at 10 mol % and 10 kDa dextran was encapsulated in the aqueous core. Hydrophilic encapsulants, such as divalent metal ions (M^{2+}) or fluorophores, were additionally incorporated within the aqueous core.

applied with precise spatial and temporal control. Light has been used in conjunction with coordination chemistry to provide a binary system that switches from caged to uncaged for both Zn^{2+} and Ca^{2+} .^{12–20} In these systems, photoactive moieties such as *o*-nitrobenzyl, fluoroionophores, and nitrodibenzofurans were used for Zn^{2+} and Ca^{2+} caging; however, high doses of near-UV light were typically required for uncaging, which limited biocompatibility and depth penetration in living tissue. Light penetration into tissue can be improved by using long wavelength irradiation that takes advantage of 1- or 2-photon excitation. NDBF-EDTA is a photosensitive calcium chelator employing a nitrodibenzofuran (NDBF) moiety shown to combine 2-photon uncaging abilities with efficient calcium binding and release.¹⁴ The NDBF 2-photon cross-section is modest (0.6 GM) as seen with other 2-photon active calcium chelators such as azid-1 and DM-nitrophen, which have 2-photon cross sections of 1.4 and 0.013 GM, respectively.²¹ There are limited examples of caging metal ions for activation with 1-photon visible (vis) or near-infrared (NIR) light. One example by Canto et al. used spiropyran receptors conjugated to single-walled carbon nanotubes (SWNTs) for the reversible trapping and release of Zn^{2+} with visible light.²²

Encapsulation within stimulus-responsive nanocarriers is a more generalizable approach to metal ion caging/release compared to ligand-caged systems.²³ The release no longer depends upon the ligand chemistry, enabling the same nanocarrier to be used for a variety of different metal ions, or to deliver a combination of metal ions simultaneously. One versatile class of nanocarriers is polymersomes, which are self-assembled bilayer vesicles synthesized from amphiphilic diblock copolymers.^{24,25} Polymersomes provide a large internal aqueous environment for hydrophilic compound encapsulation and a hyperthick membrane for hydrophobic encapsulation, and can be surface modified to provide targeting capabilities.^{26–30}

The work presented here specifically utilizes photoresponsive nanoscale polymersomes for the encapsulation and delivery of metal ions with a visible-light trigger. It has been shown, by our

laboratories and others, that it is possible to make photoresponsive polymersomes by incorporating light-responsive elements into vesicles. For example, Cabane et al. incorporated a UV-active *o*-nitrobenzyl moiety between the hydrophobic and hydrophilic polymer blocks; vesicles made from this polymer were ruptured by photolysis of this linker to release small molecular weight dyes as well as proteins.³¹ Hammer and Burdick devised a system where the photoresponsive amino acid analogue, 2-nitrophenylalanine, could be inserted in the junction of a polymersome-forming diblock copolymer; illumination caused cleavage of the polymer and the release of contents that were entrapped in the vesicle.²⁷ There are examples of other types of nanocarriers that can be made photoresponsive, such as micelles with embedded 2-photon-active photoswitches.^{32–35} Additional examples exist for controlled drug release from light-responsive nanoparticles.^{36–42}

Our laboratories have shown that micron-scale polymersomes synthesized from poly(ethylene oxide)-poly(butadiene) (OB29, MW = 3800 g/mol) can be made photoresponsive through the addition of a solute (e.g., protein or dextran) in the aqueous core and highly conjugated porphyrin-based fluorophores in the hydrophobic membrane.^{43–45} Excitation of these membrane-dispersed fluorophores with visible or NIR light results in relaxation via fluorescence and local heat generation. In conjunction with this, the aqueous solute interaction with the inner leaflet of the polymersome membrane leads to a local asymmetric membrane stretching. This results in irreversible membrane deformation and subsequent rupture.⁴⁵ Such vesicles disperse, for example, the *meso-to-meso* ethyne-bridged bis[(porphinato)zinc] (PZn_2) fluorophore, and can be engineered to undergo membrane deformation upon irradiation with vis or NIR light.

Here, we present the extension of this work from micron-scale vesicles to vesicles that are 100 to 200 nm in diameter, a size regime amenable to the use of this system in biological applications (Figure 1). Additionally, we demonstrate the ability to tune the photorelease with visible light by varying

irradiation time and the presence of dextran in the core. The system presented here shows efficient encapsulation and release of a small molecule, fluorescein isothiocyanate (FITC), and two biologically relevant metal ions, Zn^{2+} and Ca^{2+} . This is the first report of nanopolymersomes that encapsulate metal ions and release them in response to visible light.

■ EXPERIMENTAL SECTION

Self-assembly of Nanoscale Polymersomes. Nanoscale polymersomes were made by direct injection of DMSO containing poly(ethylene oxide)-polybutadiene (PEO₃₀-PBD₄₆, denoted OB29, MW = 3800 g/mol) into aqueous buffer. The final mixture contained 30% DMSO by volume and was immediately vortexed for 5 min to promote vesicle self-assembly. Vesicle size and monodispersity were tuned through polymer concentration, aqueous-to-organic volume ratio, and vortex time. To make light-responsive nanopolymersomes, PZn₂ (2123 g/mol) was added to the DMSO solution to achieve a final concentration of 10 mol % with respect to the polymer prior to vortexing.^{26,43,45–47} Dextran (10 kDa) was added to the aqueous buffer to make a 10 mg/mL solution. FITC-loaded vesicles were synthesized with a saturated solution of FITC in 290 mOsm PBS, pH 7.2. Ca^{2+} -loaded vesicles were assembled from a solution containing 150 mM CaCl₂, whereas Zn²⁺-loaded vesicles were assembled from a solution containing 150 mM ZnSO₄.

Encapsulation and Nanovesicle Purification. Hydrophilic encapsulants (dextran and FITC, or dextran and divalent metal ions) were added to the aqueous buffer prior to solvent injection and vortexing. After vortexing, vesicles were dialyzed against the corresponding buffer of equal osmolarity using a 50 kDa molecular weight cutoff dialysis cassette to remove free 10 kDa dextran and unencapsulated hydrophilic cargo. Metal ion samples were dialyzed against isosmotic NaCl for 2 days at 4 °C with at least two buffer changes. An additional separation step was performed on samples to be used for release studies to ensure that all free encapsulant was removed. A 50 kDa molecular weight cutoff Amicon Ultra centrifugal filter was used to separate any remaining free hydrophilic encapsulant from the nanovesicles. The vesicles were spun at 9300 rcf to concentrate, and resuspended in buffer for further washes. This process was repeated until free encapsulant could no longer be detected in the filtrate via UV/vis absorbance.

Vesicle Characterization. Polymersome size distribution was measured by dynamic light scattering (DLS) using a Malvern NanoZS Zetasizer. Polymersome samples were diluted 10-fold in the corresponding aqueous buffer in 1 mL polystyrene cuvettes. Vesicle size is reported as intensity %. Methods for further characterizing vesicles by cryo-TEM are detailed in the Supporting Information.

Cargo Photorelease from Polymersomes. Light-responsive polymersomes (30 μ L) were irradiated in a 3 × 3 × 5 mm³ PDMS well placed on a 0.17-micron-thick glass coverslip. An Olympus FV1000 confocal laser scanning microscope was used for irradiation, with continuous wave visible laser lines and power measured at sample (indicated in parentheses): 488 nm (25 μ W), 515 nm (21 μ W), 543 nm (19 μ W), and 633 nm (14 μ W). The laser power was set to 80% when a combination of lasers was used. When 488 nm laser excitation was used alone, the laser power was set to 100%. The sample was centered within the field of view of a 10× air objective lens (Olympus UPlanSApo, NA = 0.40), focused at the coverslip–liquid interface, and subsequently irradiated for 1, 2, 5, or 10 min without measurable sample evaporation occurring. The laser was rastered over a 512 × 512 pixel (2500 × 2500 μ m²) field of view with a dwell time of 4 μ s/pixel. A positive control (100% release) was achieved through the addition of a surfactant, Triton X-100, to a final concentration of 0.1 vol %. Negative control samples (0% release) were kept at constant osmotic strength and were not irradiated.

Detection of Cargo Release from Nanopolymersomes. After irradiation, 25 μ L of the polymersome sample was removed from the PDMS well and placed into a 50 kDa molecular weight cutoff Amicon Ultra 0.5 mL centrifugal filter and diluted to 75 μ L in the corresponding buffer. The sample was centrifuged for 15 min at

9300 rcf. The filtrate was collected and analyzed for fluorescence using a Cary Eclipse Fluorescence Spectrophotometer. The sample was placed in a small volume quartz cuvette (40 μ L) and excited at 495 nm. FITC release was calculated from the emission at 523 nm. Oregon Green 488 BAPTA-1 hexapotassium salt (Life Technologies, Grand Island, NY) (1 μ M, 5 μ L) was added to the Zn²⁺ and Ca²⁺ samples to detect the presence of these metal ions, and the peak fluorescence intensity at 517 nm was used to calculate release. Positive and negative control vesicles were subjected to the same conditions. For Ca²⁺ measurements, samples were diluted 128-fold because of the higher final metal ion concentration in solution.

Porphyrin Dimer (PZn₂) Wavelength Shift Determination. A CRi Multispectral Imaging System, NuanceFX camera attached to an Olympus IX81 inverted microscope, was used for measurement of the PZn₂ emission spectrum before and after sample irradiation. Epi-fluorescence illumination was used for PZn₂ excitation with a mercury-arc lamp and 530–550 nm band-pass filter. A three-dimensional image cube, measuring PZn₂ emission from 660–720 nm in 3 nm steps, was collected by the camera through a 10× air objective (Olympus UPlanSApo, NA = 0.40). The PZn₂ emission spectrum was determined for select regions of interest using the Nuance 2.10 real component analysis software.

In Vivo PZn₂ Emission Wavelength Shift Determination. Zebrafish embryos were obtained from the CDB Zebrafish Core Facility at the University of Pennsylvania, Perelman School of Medicine. All embryos obtained were Tübingen Long-Fin (TLF × TLF) wild-type. Nanopolymersomes were made according to the aforementioned protocol with PZn₂ (10 mol %) in the hydrophobic membrane and dextran in the aqueous core (10 kDa, 10 mg/mL). For in vivo imaging and toxicity experiments, vesicles were prepared with 10 kDa Texas Red Dextran in the aqueous core. Nanopolymersome samples were concentrated 4-fold from the initial preparation (to final concentration = 1.2 mM OB29) and injected without further modification. A Harvard Apparatus PLI-100 Pico-Injector was used to inject controlled volumes. Injection volume was calibrated to dispense 10 nL per embryo. All injections were performed at the one-cell stage and injected only into the cell compartment. Zebrafish embryos were incubated at 28 °C in E3 zebrafish medium and imaged at the 1-cell stage and at later stages extending to 30 h postfertilization (hpf). Embryo micrographs were collected with an Olympus FV1000 laser scanning confocal microscope using transmitted light imaging and fluorescence imaging. A 10× air objective (Olympus UPlanSApo, NA = 0.40) was used for single embryo imaging and irradiation. For PZn₂ emission shift determination, a region of interest (ROI) was selected to include the cellular compartment only, and irradiated with 488 nm for 5 min. A CRi Multispectral Imaging System, NuanceFX camera attached to an Olympus IX81 inverted microscope was used for measurement of the PZn₂ emission spectrum before and after embryo irradiation. Epi-fluorescence illumination was used for PZn₂ excitation with a mercury-arc lamp and 530–550 nm band-pass filter. A three-dimensional image cube measuring PZn₂ emission from 660–720 nm in 3 nm steps was collected by the camera through a 10× air objective (Olympus UPlanSApo, NA = 0.40). The PZn₂ emission spectrum was determined for the ROI using Nuance 2.10 real component analysis software pre- and post-irradiation.

Materials. PEO₃₀-PBD₄₆ (OB29) was purchased from Polymer Source (Quebec, Canada). Oregon Green 488 BAPTA-1 hexapotassium salt was purchased from Life Technologies (Grand Island, NY). PBS (10×), DMSO (ACS reagent grade), CaCl₂ (dihydrate), ZnSO₄ (heptahydrate), and Slide-a-lyzer G2 dialysis cassettes, were purchased from Fisher Scientific (Pittsburgh, PA). Amicon Ultra centrifugal filters were purchased from Millipore (Billerica, MA). Texas Red Dextran, 10 000 MW, was purchased from Life Technologies (Grand Island, NY).

■ RESULTS AND DISCUSSION

Vesicle Self-Assembly Characterization. In previous reports, OB29 nanopolymersomes were made through thin-film self-assembly, where polymer was dried onto a Teflon square

and subsequently incubated with the hydration solution and vortexed to make nanovesicles.^{26,28} This method limits the maximum concentration of polymer that can be cast onto the Teflon square to that required to make an even film, which reduces the vesicle yield and consequently the amount of cargo that can be encapsulated. To increase the concentration of polymer (and vesicle yield), a direct solvent injection method of self-assembly was explored where OB29 in DMSO was directly injected into PBS buffer, and immediately vortexed to promote self-assembly. Polymer concentration, DMSO percentage, and vortex time were varied to determine the best conditions for the self-assembly of monodisperse, unilamellar nanovesicles using OB29 polymer. The assembly conditions were carefully chosen to maximize spherical vesicle formation with limited nonvesicular structures.⁴⁸ OB29 was selected due to its innate stability toward pH and temperature changes, as well as low membrane permeability once assembled into a vesicle.⁴⁹ The concentration of polymer in DMSO was varied from 1 to 3 mM and vesicle sizes were analyzed by DLS and confirmed by cryo-TEM (Supporting Information Figure S1). The ratio of DMSO to aqueous buffer was optimized as well, ranging from 10% to 70% final volume of DMSO in buffer (Supporting Information Figures S2, S3). Additionally, the promotion of self-assembly was compared with vortex times of 1, 5, 10, and 20 min (Supporting Information Figures S4, S5). Through testing various conditions, it was determined that 1.5 mM OB29 in DMSO, directly injected into 0.1 M PBS at a 30/70% v/v ratio, immediately followed by 5 min vortexing, yielded a large population of monodisperse, unilamellar vesicles. Vesicles from these conditions were determined by dynamic light scattering to have an average hydrodynamic diameter of 120 ± 20 nm (Supporting Information Figure S6). To make the vesicles light responsive, identical conditions were used with DMSO solutions of OB29 containing 10 mol % PZn₂ and vesicles were again analyzed by DLS and imaged by cryo-TEM. Figure 2 shows the histogram of vesicle diameters at the final self-assembly conditions, centered at 140 nm, and the morphology of the PZn₂-loaded nanovesicles as seen by cryo-TEM.

Nanovesicle Rupture Determined by PZn₂ Emission Shift. The *meso-to-meso* ethyne-bridged (porphinato)zinc(II) fluorophore (PZn₂, Supporting Information Figure S7) was previously demonstrated to undergo an emission band shift in response to its environment; deformation of micron-scale OB29 vesicles was monitored by this approach.⁵⁰ We expect PZn₂ to adopt similar conformations within nano- and micron-polymersomes as the thickness of the OB29 hydrophobic membrane is the same in these vesicles.⁵¹ Encapsulation within the polymersome membrane at high loading restricts the mean PZn-PZn torsional angle, causing PZn₂ to adopt a more planar structure and exhibit a red-shifted emission band compared to that observed in dilute solution.⁵⁰ Upon irradiation (488 nm) and membrane destabilization, PZn₂ encounters more free volume within the membrane, which drives an increase in its mean interplanar torsional angle, causing a fluorescence blue-shift relative to that observed for unirradiated polymersomes.⁵⁰ Thus, PZn₂ emission wavelength is a convenient and accurate way to monitor vesicle integrity and rupture.

To probe nanovesicle rupture, vesicles were irradiated with visible light (488, 515, 543, 633 nm) for increasing amounts of time (1, 5, 10, 20 min). A multispectral imaging camera was used to determine an aggregate PZn₂ emission of the bulk polymersome-containing solution after each irradiation period.

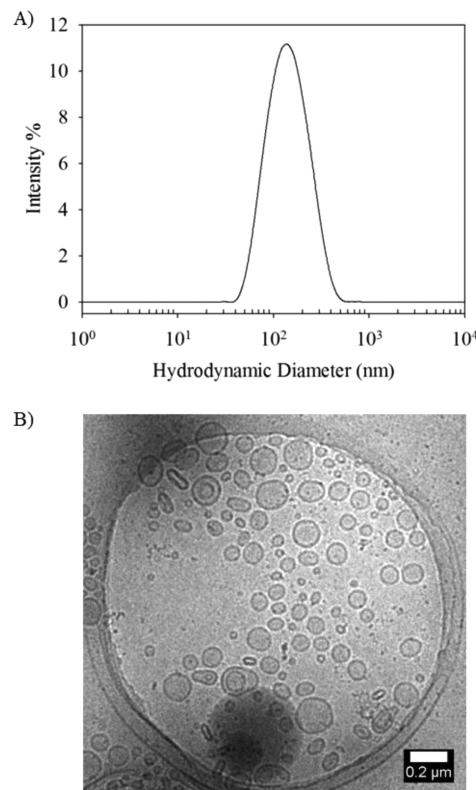


Figure 2. Polymersome characterization. (A) Size distribution of polymersomes in (B) as determined by dynamic light scattering. (B) Cryo-TEM image of polymersomes containing 10 mol % PZn₂ in the membrane. Scale bar indicates 200 nm.

PZn₂ emission blue-shifted from 714 to 705 nm with increasing irradiation times (Figure 3A), consistent with PZn₂ adopting a more twisted structure in a less conformationally restricted environment (Figure 3B). The sample irradiated for 20 min correlated well with a positive control release sample where a surfactant, Triton X-100, was added to fully destabilize the membrane. These data were consistent with vesicle rupture.

FITC Loading and Release from Nanovesicles. Initially, we investigated this photoresponsive nanopolymersome system by encapsulating and releasing a model hydrophilic dye molecule, fluorescein isothiocyanate (FITC). The photo-response of the nanopolymersomes was investigated in response to dextran, irradiation time, and irradiation sources. Previous work from our laboratories developed a generalized system for tuning the photoresponsiveness of micron-sized polymersomes.⁴⁵ It was determined that including a high molecular weight dextran in the aqueous core of polymersomes and PZn₂ in the membrane was required for vesicle rupture. Previously, we provided multiple lines of evidence that dextran likely interacts with the inner leaflet of the bilayer membrane and reduces its elasticity, whereas nonradiative relaxation pathways of electronically excited PZn₂ function to generate local heating upon irradiation.^{45,50} The combined effect produces an asymmetric thermal stretching of the membrane, ultimately causing rupture.⁴⁵ We translated these findings to photoresponsive nanovesicles, with a modification to encapsulate lower molecular weight dextran (10 kDa) in the aqueous core due to the smaller luminal volume of nanopolymersomes. It was also hypothesized that the membrane could be

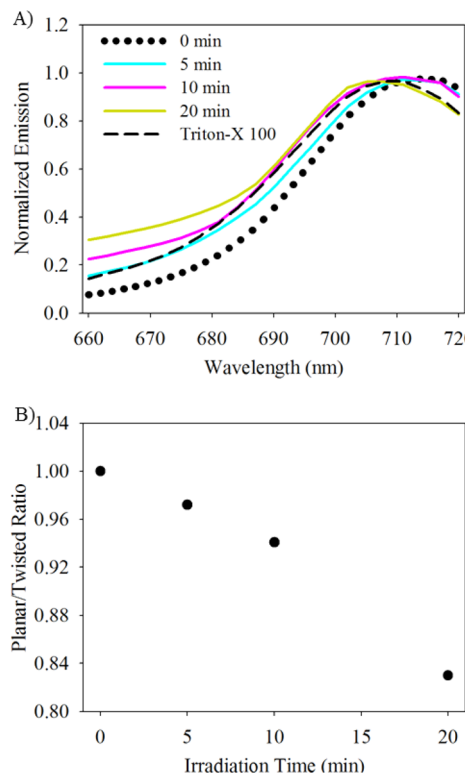


Figure 3. Membrane deformation detected by PZn_2 emission blue-shift. (A) Emission spectrum for PZn_2 in nanopolymersomes was detected as a function of irradiation time. The emission blue-shifted with increasing irradiation time. (B) Normalized ratio of I_{714} (more planar) to I_{705} (more twisted conformations).

destabilized from the thermal expansion caused by PZn_2 alone because of the increased curvature of nanovesicles.

To assess the dependence of triggered release upon the presence of dextran, FITC was loaded into the aqueous core of nanopolymersomes with and without the inclusion of 10 kDa dextran in the aqueous core. Both systems were irradiated with a 488 nm laser, or via a combination of four visible wavelength lasers (488, 515, 543, 633 nm). The combination of four lasers was chosen as an extension of our previous work with micron-vesicles, corresponding to several absorbance features of PZn_2 in the polymersome membrane.⁴⁵ The 488 nm laser was chosen as a single irradiation source as PZn_2 absorbs maximally near this wavelength. The release curves for these four conditions (+/- dextran, 488 nm/all lasers) are shown in Figure 4. As expected, percent release (calculated from Supporting Information Equation S1) was identical within experimental error when using 488 nm excitation only (Figure 4B) vs the combination of simultaneous excitation using all visible laser light sources (Figure 4D). This provided additional evidence that vesicle rupture was due to PZn_2 absorption and not a nonspecific effect of irradiation, as the combined laser power was significantly greater than 488 nm alone. As hypothesized, due to the increased curvature, nanopolymersomes ruptured without dextran (Figure 4A,C), contrary to the previous micron-vesicle polymersome system. Nonetheless, dextran-loaded nanovesicles consistently exhibited higher % release under all conditions tested (Figure 4). Nanopolymersomes were also prepared without PZn_2 and dextran, and maximum irradiation of these vesicles resulted in negligible FITC release (Supporting Information Figure S8), which confirmed the need for PZn_2 .

To better understand the mechanism of rupture, nanopolymersomes were imaged by cryo-TEM before and after irradiation (Figure 5). Figure 5A shows a large population of uniform, unilamellar vesicles before irradiation as well as a small number of worm-like micelles. After irradiation, many non-vesicular structures were present (Figure 5B) including a larger

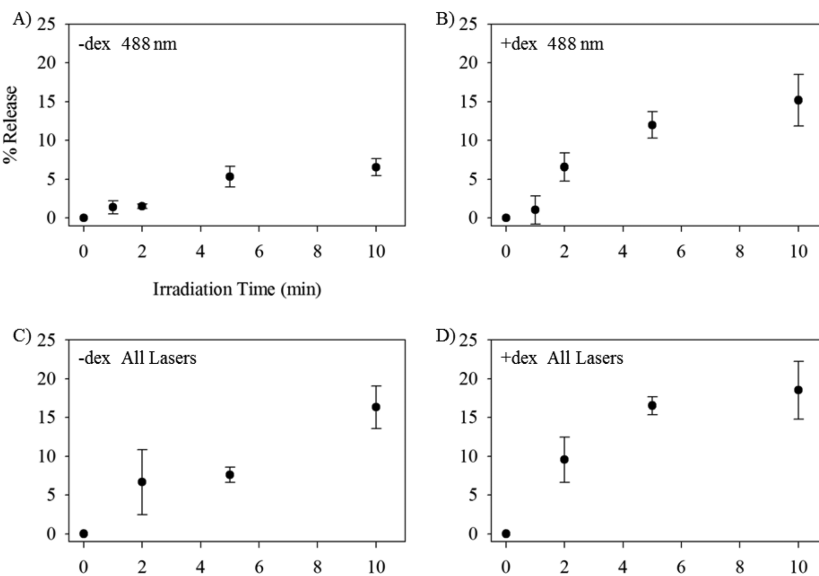


Figure 4. Release curve of FITC-loaded polymersomes. Nanopolymersomes containing PZn_2 in their membranes were irradiated for various amounts of time. (A) Polymersomes containing no dextran in the core ($\lambda_{\text{ex}} = 488 \text{ nm}$; see Experimental Section for details regarding the light source and excitation conditions). (B) Polymersomes containing 10 kDa dextran in the core and irradiated with 488 nm laser. (C) Polymersomes containing no dextran in the core and simultaneously irradiated using 488, 515, 543, and 633 nm laser light sources. (D) Polymersomes containing 10 kDa dextran in the core and simultaneously irradiated using 488, 515, 543, and 633 nm laser light sources. Each point represents the average of 3 trials +/- SEM.

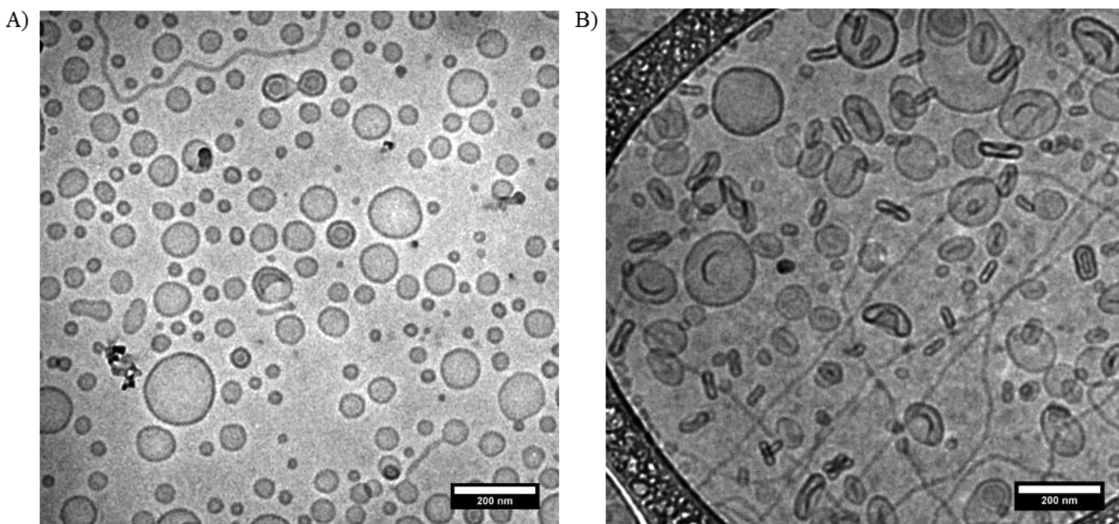


Figure 5. Morphological change in polymersomes after light irradiation. Polymersomes containing 10 mol % PZn₂ in the membrane and 10 kDa dextran and FITC in the core were imaged with cryo-TEM: (A) before irradiation, and (B) after 20 min of simultaneous irradiation using 488, 515, 543, and 633 nm laser light sources. Scale bars indicate 200 nm.

fraction of worm-like micelles and “dumbbell”-shaped vesicles. These images suggest a rupture mechanism where the membrane buckles and folds over itself, or is disrupted and reassembles. The mechanism was further corroborated by DLS, which showed no significant change in size post-irradiation.

In Vivo Nanovesicle Rupture Determined by PZn₂ Emission Shift. Experiments were performed in living zebrafish embryos to determine the ability to rupture nanovesicles in vivo. Zebrafish embryos were injected at the 1-cell stage with nanopolymersomes containing PZn₂ in the hydrophobic membrane and dextran in the aqueous core. The emission wavelength of PZn₂ was measured within the cellular compartment of the embryo before and after 488 nm irradiation (rastering the ROI for 5 min). The embryos were imaged before (Figure 6A) and after irradiation (Figure 6B) to confirm that no physical damage occurred to the embryo during the irradiation process. An identical blue-shift in emission from 714 to 705 nm was detected in vivo as was seen in the bulk sample (Figure 3A,B). The complete shift to 705 nm was seen with significantly less irradiation time in vivo than in the bulk sample (5 min vs 20 min), likely due to the smaller volume being irradiated. To investigate nanopolymerosome toxicity and diffusion within a living zebrafish embryo, nanovesicles containing membrane-dispersed PZn₂ and Texas Red-dextran (MW = 10 kDa) in the aqueous cores were microinjected at the 1-cell stage. Embryos were monitored for PZn₂ and Texas Red emission, as well as normal development from the 1-cell stage up through 30 hpf (Supporting Information Figure S9). Embryos developed normally, comparable to the uninjected controls. Emission from PZn₂ and Texas Red could be detected until 30 hpf, at which point the increased volume of the developing embryo likely diluted the signal.

Loading and Releasing Metal Ions with Photo-responsive Nanopolymersomes. To demonstrate the versatility of this system, encapsulation and release techniques were applied to two metal ions with importance in cellular processes. Ca²⁺ or Zn²⁺ was incorporated into the aqueous core of nanopolymersomes via an identical direct-injection self-assembly process that utilized a 150 mM metal ion solution.

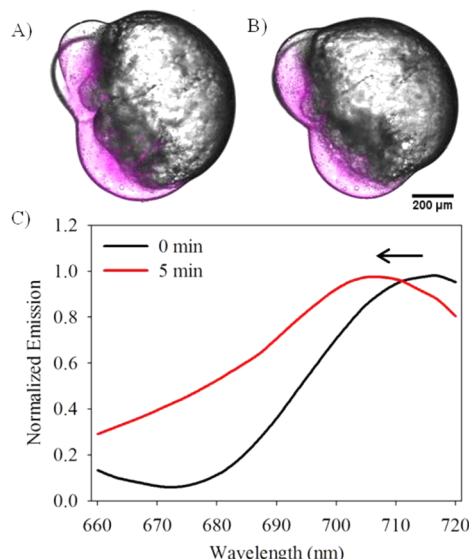


Figure 6. Nanopolymersome rupture in vivo detected by PZn₂ emission blue-shift. (A) Representative image of zebrafish embryo microinjected with nanopolymersomes and imaged at the 4-cell stage. (B) Injected embryo was irradiated with 488 nm laser for 5 min and imaged. Scale bar is 200 microns. (C) Emission spectra of PZn₂ in nanopolymersomes were measured within the cellular compartment of the embryo before (black) and after (red) irradiation.

Building on the results detailed in Figures 4 and 5, these vesicles were prepared with 10 kDa dextran in the aqueous core and 10 mol % PZn₂ in the hydrophobic membrane and characterized by DLS (Supporting Information Figure S10). Metal ion-loaded vesicles were subjected to varying irradiation times using 488 nm excitation. Figure 7 shows release curves for Ca²⁺ (A) and Zn²⁺ (B). Both metal ions were successfully loaded and released from nanopolymersomes, with maximum release occurring for both ions within 10 min irradiation of the polymersome solution.

The concentration jump of Ca²⁺ in solution after vesicle rupture was determined to be 760 μM and the concentration of Zn²⁺ in solution after vesicle rupture was 35 μM. Both

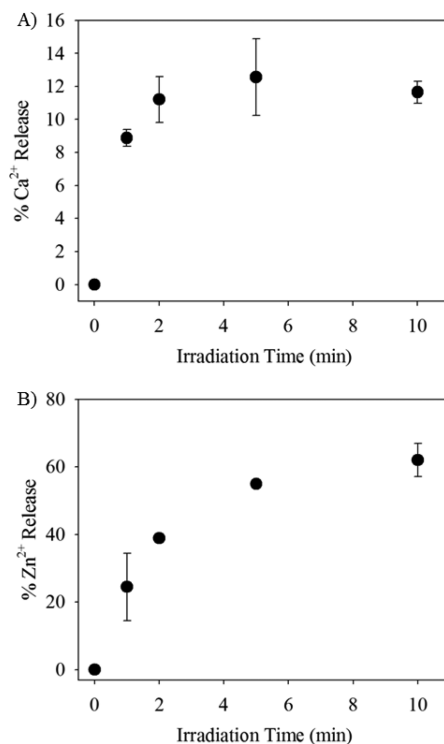


Figure 7. Release curves of metal ion-loaded polymersomes. Nanopolymersomes containing PZn₂ in the membrane were irradiated for various amounts of time. (A) Ca²⁺-loaded polymersomes. (B) Zn²⁺-loaded polymersomes. Each point represents the average of 3 trials +/− SEM.

concentration values were determined by full release from vesicles with Triton X-100 and quantified via corresponding Oregon Green-488 BAPTA-1 calibration curves. The final concentration of OB29 polymer in the irradiation sample was kept constant at 0.3 mM, and the number of vesicles per sample volume was assumed to be consistent. The average number of 130 000 Ca²⁺ ions per vesicle and 6000 Zn²⁺ ions per vesicle was estimated assuming a polymer density of 1 chain/nm², which has previously been used to calculate vesicle number (Supporting Information Equation S2).²⁸ Differences in Ca²⁺ and Zn²⁺ vesicle loading may result, in part, from counterion effects (Cl[−] vs SO₄^{2−}) of the metal salts employed. Although the concentration of released Zn²⁺ was significantly lower than the level achieved with Ca²⁺, it is still appropriate for biological applications, as the cellular concentration of free Zn²⁺ is typically in the picomolar to nanomolar range.⁵²

Currently, DM-nitrophen (Millipore, Billerica, MA) is the most efficient caged Ca²⁺ chelator, based on its high calcium affinity before photolysis, and low affinity postphotolysis. Upon irradiation with UV light (365 nm), DM Nitrophen can provide up to a 600 μM jump in Ca²⁺ concentration in living neurons.¹⁶ However, DM Nitrophen must be employed at similarly high concentration due to the monovalency of the chelator. As noted above, the nanopolymersome system can provide a similar Ca²⁺ concentration jump, with the added benefits of visible-light release, potential for greater biological stability, and the ability to encapsulate tens of thousands of ions per vesicle. Further optimization of nanopolymersomes may be possible, for example, to accelerate the rate and % yield of metal ion release.

CONCLUSIONS

We have reported a visible light-responsive nanopolymerosome system capable of encapsulating and releasing small molecules (FITC) and metal ions (Ca²⁺ and Zn²⁺). The nanopolymerosomes could be detected in developing zebrafish embryos until 30 hpf, and were additionally shown to be photoresponsive *in vivo*. This system encapsulated the hydrophobic ethyne-bridged bis[(porphinato)zinc] fluorophore in the membrane to provide thermal expansion and subsequent membrane rupture upon optical excitation. Inclusion of dextran in the aqueous core increased loading and fractional release; however, rupture was also achieved without dextran, unlike our previously reported micron-sized photoresponsive polymerosomes, perhaps due to the increased curvature of the nanovesicles and a corresponding increased sensitivity to localized heating driven by nonradiative relaxation of the membrane-dispersed electronically excited PZn₂ chromophore.⁴⁵

Importantly, we demonstrated metal ion release at concentrations suitable for cellular applications. Our system has many potential benefits over previously reported caged chelators, namely, the use of 488 nm light, and the ability to encapsulate different metal ions without the need for modifying metal chelation or changing the self-assembly process. Our results in living zebrafish embryos along with previous reports of passive uptake in cells make this system advantageous for *in vivo* delivery.⁵³ Additionally, encapsulation within polymerosomes increased the mean residence time of cargo *in vivo* in comparison to uncaged systems.⁵⁴ The PZn₂ emission shift provided a built-in reporter for vesicle rupture, which was useful for monitoring vesicle deformation in solution or in living zebrafish embryos. Additionally, due to the broad absorbance spectrum of PZn₂, it is feasible to extend future work to releasing with near-IR light, as PZn₂ has an absorption manifold centered at ~700 nm,²⁶ or through the use of related fluorophores that are dispersible within the polymerosome membrane and emit at longer wavelengths.^{26,43}

ASSOCIATED CONTENT

S Supporting Information

Details on self-assembly variables, structure of PZn₂, *in vivo* image collection, DLS of metal ion-containing vesicles, and additional methods. This material is available free of charge via the Internet at <http://pubs.acs.org>.

AUTHOR INFORMATION

Corresponding Author

*E-mail: ivandmo@sas.upenn.edu.

Author Contributions

Julianne C. Griepenburg and Nimil Sood contributed equally.

Notes

The authors declare no competing financial interest.

ACKNOWLEDGMENTS

This work was supported by National Institutes of Health R01 GM083030 to I.J.D. M.J.T. and J.R. acknowledge Department of Defense (W81XWH-13-1-0086) for financial support. The effort of D.A.H., N.S., and K.B.V. (making vesicles, photo-release, and cryo-TEM) was supported by the Biomolecular Materials program at the U. S. Department of Energy, Office of Basic Energy Science, Division of Materials Science (DE-

FG02–11ER46810). Olympus FV1000 confocal microscope was supported by NIH 1S10RR021113.

■ REFERENCES

- (1) Bush, A. I. Metals and neuroscience. *Curr. Opin. Chem. Biol.* **2000**, *4*, 184–191.
- (2) King, J. C.; Shames, D. M.; Woodhouse, L. R. Zinc homeostasis in humans. *J. Nutr.* **2000**, *130*, 1360S–1366S.
- (3) Takeda, A. Zinc homeostasis and functions of zinc in the brain. *Biometals* **2001**, *14*, 343–351.
- (4) Kaur, K.; Gupta, R.; Saraf, S. A.; Saraf, S. K. Zinc: The metal of life. *Compr. Rev. Food Sci. Food Saf.* **2014**, *13*, 358–376.
- (5) Carafoli, E. Intracellular calcium homeostasis. *Annu. Rev. Biochem.* **1987**, *56*, 395–433.
- (6) Minta, A.; Kao, J. P.; Tsien, R. Y. Fluorescent indicators for cytosolic calcium based on rhodamine and fluorescein chromophores. *J. Biol. Chem.* **1989**, *264*, 8171–8178.
- (7) Komatsu, K.; Kikuchi, K.; Kojima, H.; Urano, Y.; Nagano, T. Selective zinc sensor molecules with various affinities for Zn²⁺, revealing dynamics and regional distribution of synaptically released Zn²⁺ in hippocampal slices. *J. Am. Chem. Soc.* **2005**, *127*, 10197–10204.
- (8) Domaille, D. W.; Que, E. L.; Chang, C. J. Synthetic fluorescent sensors for studying the cell biology of metals. *Nat. Chem. Biol.* **2008**, *4*, 168–175.
- (9) Haas, K. L.; Franz, K. J. Application of metal coordination chemistry to explore and manipulate cell biology. *Chem. Rev.* **2009**, *109*, 4921–4960.
- (10) Tomat, E.; Lippard, S. J. Imaging mobile zinc in biology. *Curr. Opin. Chem. Biol.* **2010**, *14*, 225–230.
- (11) Mbatia, H. W.; Burdette, S. C. Photochemical tools for studying metal ion signaling and homeostasis. *Biochemistry* **2012**, *51*, 7212–7224.
- (12) Tsien, R. Y.; Zucker, R. S. Control of cytoplasmic calcium with photolabile tetracarboxylate 2-nitrobenzhydrol chelators. *Biophys. J.* **1986**, *50*, 843–853.
- (13) Marcotte, N.; Plaza, P.; Lavabre, D.; Fery-Forgues, S.; Martin, M. M. Calcium photorelease from a symmetrical donor-acceptor-donor bis-crown-fluoroionophore evidenced by ultrafast absorption spectroscopy. *J. Phys. Chem. A* **2003**, *107*, 2394–2402.
- (14) Momotake, A.; Lindeger, N.; Niggli, E.; Barsotti, R. J.; Ellis-Davies, G. C. R. The nitrodibenzofuran chromophore: a new caging group for ultra-efficient photolysis in living cells. *Nat. Methods* **2006**, *3*, 35–40.
- (15) Ellis-Davies, G. C. Caged compounds: photorelease technology for control of cellular chemistry and physiology. *Nat. Methods* **2007**, *4*, 619–628.
- (16) Ellis-Davies, G. C. R. Neurobiology with caged calcium. *Chem. Rev.* **2008**, *108*, 1603–1613.
- (17) Bandara, H. M.; Kennedy, D. P.; Akin, E.; Incarvito, C. D.; Burdette, S. C. Photoinduced release of Zn²⁺ with ZinCleav-1: A nitrobenzyl-based caged complex. *Inorg. Chem.* **2009**, *48*, 8445–8455.
- (18) Zhang, X.; Chen, Y. Photo-controlled Zn²⁺ release system with dual binding-sites and turn-on fluorescence. *Phys. Chem. Chem. Phys.* **2010**, *12*, 1177–1181.
- (19) Ciesienski, K. L.; Franz, K. J. Keys for unlocking photolabile metal-containing cages. *Angew. Chem., Int. Ed.* **2011**, *50*, 814–824.
- (20) Gwizdala, C.; Basa, P. N.; MacDonald, J. C.; Burdette, S. C. Increasing the dynamic range of metal ion affinity changes in Zn²⁺ photocages using multiple nitrobenzyl groups. *Inorg. Chem.* **2013**, *52*, 8483–8494.
- (21) Brown, E. B.; Shear, J. B.; Adams, S. R.; Tsien, R. Y.; Webb, W. W. Photolysis of caged calcium in femtoliter volumes using two-photon excitation. *Biophys. J.* **1999**, *76*, 489–499.
- (22) Canto, E. D.; Natali, M.; Movia, D.; Giordani, S. Photocontrolled release of zinc metal ions by spiropyran receptors anchored to single-walled carbon nanotubes. *Phys. Chem. Chem. Phys.* **2012**, *14*, 6034–6043.
- (23) Fomina, N.; Sankaranarayanan, J.; Almutairi, A. Photochemical mechanisms of light-triggered release from nanocarriers. *Adv. Drug Delivery Rev.* **2012**, *64*, 1005–1020.
- (24) Discher, B. M.; Won, Y. Y.; Ege, D. S.; Lee, J. C. M.; Bates, F. S.; Discher, D. E.; Hammer, D. A. Polymersomes: Tough vesicles made from diblock copolymers. *Science* **1999**, *284*, 1143–1146.
- (25) Lee, J. S.; Feijen, J. Polymersomes for drug delivery: design, formation and characterization. *J. Controlled Release* **2012**, *161*, 473–483.
- (26) Ghoroghchian, P. P.; Frail, P. R.; Susumu, K.; Blessington, D.; Brannan, A. K.; Bates, F. S.; Chance, B.; Hammer, D. A.; Therien, M. J. Near-infrared-emissive polymersomes: Self-assembled soft matter for in vivo optical imaging. *Proc. Natl. Acad. Sci. U. S. A.* **2005**, *102*, 2922–2927.
- (27) Katz, J. S.; Zhong, S.; Ricart, B. G.; Pochan, D. J.; Hammer, D. A.; Burdick, J. A. Modular synthesis of biodegradable diblock copolymers for designing functional polymersomes. *J. Am. Chem. Soc.* **2010**, *132*, 3654–3655.
- (28) Christian, N. A.; Milone, M. C.; Ranka, S. S.; Li, G.; Frail, P. R.; Davis, K. P.; Bates, F. S.; Therien, M. J.; Ghoroghchian, P. P.; June, C. H.; Hammer, D. A. Tat-functionalized near-infrared emissive polymersomes for dendritic cell labeling. *Bioconjugate Chem.* **2007**, *18*, 31–40.
- (29) Demirgöz, D.; Pangburn, T. O.; Davis, K. P.; Lee, S.; Bates, F. S.; Kokkoli, E. PR_b-targeted delivery of tumor necrosis factor- α by polymersomes for the treatment of prostate cancer. *Soft Matter* **2009**, *5*, 2011–2019.
- (30) Zupancich, J. A.; Bates, F. S.; Hillmyer, M. A. Synthesis and self-assembly of RGD-functionalized PEO-PB amphiphiles. *Biomacromolecules* **2009**, *10*, 1554–1563.
- (31) Cabane, E.; Malinova, V.; Menon, S.; Palivan, C. G.; Meier, W. Photoresponsive polymersomes as smart, triggerable nanocarriers. *Soft Matter* **2011**, *7*, 9167–9176.
- (32) Zhang, Q.; Ko, N. R.; Oh, J. K. Modulated morphologies and tunable thiol-responsive shedding of aqueous block copolymer aggregates. *RSC Adv.* **2012**, *2*, 8079–8086.
- (33) Zhang, X.; Chen, Y. Photo-controlled metal-ion (Zn²⁺ and Cd²⁺) release in aqueous Tween-20 micelle solution. *Phys. Chem. Chem. Phys.* **2012**, *14*, 2312–2316.
- (34) Chen, C.-J.; Liu, G.-Y.; Liu, X.-S.; Li, D.-D.; Ji, J. Construction of photo-responsive micelles from azobenzene-modified hyperbranched polyphosphates and study of their reversible self-assembly and disassembly behaviours. *New J. Chem.* **2012**, *36*, 694–701.
- (35) Olejniczak, J.; Sankaranarayanan, J.; Viger, M. L.; Almutairi, A. Highest efficiency two-photon degradable copolymer for remote controlled release. *ACS Macro Lett.* **2013**, *2*, 683–687.
- (36) Jiang, J.; Tong, X.; Morris, D.; Zhao, Y. Toward photocontrolled release using light-dissociable block copolymer micelles. *Macromolecules* **2006**, *39*, 4633–4640.
- (37) Fomina, N.; McFearin, C.; Sermsakdi, M.; Edigin, O.; Almutairi, A. UV and near-IR triggered release from polymeric nanoparticles. *J. Am. Chem. Soc.* **2010**, *132*, 9540–9542.
- (38) Cong, L. V.; Wang, Z.; Wang, P.; Tang, X. J. Photodegradable polyurethane self-assembled nanoparticles for photocontrollable release. *Langmuir* **2012**, *28*, 9387–9394.
- (39) Liu, X.; Tian, Z.; Chen, C.; Allcock, H. R. UV-cleavable unimolecular micelles: synthesis and characterization toward photo-controlled drug release carriers. *Polym. Chem.* **2013**, *4*, 1115–1125.
- (40) Bansal, A.; Zhang, Y. Photocontrolled nanoparticle delivery systems for biomedical applications. *Acc. Chem. Res.* **2014**, *47*, 3052–3060.
- (41) Barman, S.; Mukhopadhyay, S. K.; Behara, K. K.; Dey, S.; Singh, N. D. P. 1-acetylpyrene–salicylic acid: photoresponsive fluorescent organic nanoparticles for the regulated release of a natural antimicrobial compound, salicylic acid. *ACS Appl. Mater. Interfaces* **2014**, *6*, 7045–7054.
- (42) Xing, Q.; Li, N.; Chen, D.; Sha, W.; Jiao, Y.; Qi, X.; Xu, Q.; Lu, J. Light-responsive amphiphilic copolymer coated nanoparticles as nanocarriers and real-time monitors for controlled drug release. *J. Mater. Chem. B* **2014**, *2*, 1182–1189.

- (43) Ghoroghchian, P. P.; Frail, P. R.; Susumu, K.; Park, T.-H.; Wu, S. P.; Uyeda, H. T.; Hammer, D. A.; Therien, M. J. Broad spectral domain fluorescence wavelength modulation of visible and near-infrared emissive polymersomes. *J. Am. Chem. Soc.* **2005**, *127*, 15388–15390.
- (44) Robbins, G. P.; Jimbo, M.; Swift, J.; Therien, M. J.; Hammer, D. A.; Dmochowski, I. J. Photoinitiated destruction of composite porphyrin–protein polymersomes. *J. Am. Chem. Soc.* **2009**, *131*, 3872–3874.
- (45) Kamat, N. P.; Robbins, G. P.; Rawson, J.; Therien, M. J.; Dmochowski, I. J.; Hammer, D. A. A generalized system for photoresponsive membrane rupture in polymersomes. *Adv. Funct. Mater.* **2010**, *20*, 2588–2596.
- (46) Duncan, T. V.; Susumu, K.; Sinks, L. E.; Therien, M. J. Exceptional near-infrared fluorescence quantum yields and excited-state absorptivity of highly conjugated porphyrin arrays. *J. Am. Chem. Soc.* **2006**, *128*, 9000–9001.
- (47) Lin, V. S.-Y.; DiMagno, S. G.; Therien, M. J. Highly conjugated, acetylenyl bridged porphyrins: new models for light-harvesting antenna systems. *Science* **1994**, *264*, 1105–1111.
- (48) Jain, S.; Bates, F. S. On the origins of morphological complexity in block copolymer surfactants. *Science* **2003**, *300*, 460–464.
- (49) Onaca, O.; Enea, R.; Hughes, D. W.; Meier, W. Stimuli-responsive polymersomes as nanocarriers for drug and gene delivery. *Macromol. Biosci.* **2009**, *9*, 129–139.
- (50) Kamat, N. P.; Liao, Z.; Moses, L. E.; Rawson, J.; Therien, M. J.; Dmochowski, I. J.; Hammer, D. A. Sensing membrane stress with near IR-emissive porphyrins. *Proc. Natl. Acad. Sci. U. S. A.* **2011**, *108*, 13984–13989.
- (51) Bermudez, H.; Brannan, A. K.; Hammer, D. A.; Bates, F. S.; Discher, D. E. Molecular weight dependence of polymersome membrane structure, elasticity, and stability. *Macromolecules* **2002**, *4*, 8203–8208.
- (52) Stork, C. J.; Li, Y. V. Zinc release from thapsigargin/IP3-sensitive stores in cultured cortical neurons. *J. Mol. Signal* **2010**, *5*, 1–6.
- (53) Anraku, Y.; Kishimura, A.; Kobayashi, A.; Oba, M.; Kataoka, K. Size-controlled long-circulating PICsome as a ruler to measure critical cut-off disposition size into normal and tumor tissues. *Chem. Commun.* **2011**, *47*, 6054–6056.
- (54) Lee, J. S.; Ankone, M.; Pieters, E.; Schiffelers, R. M.; Hennink, W. E.; Feijen, J. Circulation kinetics and biodistribution of dual-labeled polymersomes with modulated surface charge in tumor-bearing mice: comparison with stealth liposomes. *J. Controlled Release* **2011**, *155*, 282–288.